

# EFFECT OF DIELECTRIC PROPERTIES AND A TRANSVERSE DIMENSION OF CYLINDRICAL PARTICLES ON DEPOLARIZATION OF A LIDAR SIGNAL

R.F. Rakhimov and D.N. Romashov

*Institute of Atmospheric Optics,  
Siberian Branch of the Russian Academy of Sciences, Tomsk  
Received January 27, 1992*

*Effect of dielectric characteristics and the radius of circular cylindrical particles on the lidar return formation for linearly polarized sounding radiation is analyzed based on numerical model estimates. Some results of model calculations for polydisperse ensembles of ice crystals and soot particles with typical transverse radii  $r_m = 0.1-16 \mu\text{m}$  are presented. The estimates are given for the radiation wavelengths  $\lambda = 1.06$  and  $10.6 \mu\text{m}$ . The elements of a scattering phase matrix for randomly oriented circular cylinders of a finite length are compared with analogous elements for chaotically oriented elongated spheroids is for the purpose of testing the algorithm.*

The development of means for optical diagnostics of the atmospheric processes has arisen the problem on providing these means with data on the light-scattering properties of the aerosol component of the atmosphere. The problem on light scattering by nonspherical particles attracts closer attention of researchers since the optical response from such particles bears much more information about their properties as well as about the state of a carrier-medium.

The approaches based on the results of a rigorous (exact) solution of the boundary value problem of electromagnetic wave scattering are widely used in the theoretical analysis of the problem on light scattering by nonspherical particles. These are such approaches as a method of separation of variables, a method of  $T$ -matrices<sup>2</sup> as well as some approximate methods, which are quite correct in certain limiting cases.

A circular cylinder of a finite length (CCFL) is the most simple nonspherical particle. For particles of such a shape there exists an approximate solution of the light-scattering problem,<sup>3,4</sup> under the only limiting condition that  $l \gg r$ , where  $l$  is the length and  $r$  is the radius of the cylinder. It should be noted that for particles of an elongated shape the light-scattering parameters depend on the following factors:

- (a) refractive index of the particulate matter,
- (b) typical dimensions (the length  $l$  and the diameter  $d$  of a CCFL and semimajor  $a$  and semiminor  $b$  axes of an elongated spheroid (ES), and
- (c) degree of a preferred orientation of the elongation axis.

The purpose of this paper is to compare elements of the scattering phase matrix of an ensemble of the chaotically oriented CCFL with the elements<sup>8</sup> for the equivolume ES, as well as to analyze the contribution of the first two factors to the lidar return formation. The influence of the last of the above-mentioned factors has been studied in Ref. 4.

## 1. ELEMENTS OF SCATTERING PHASE MATRIX FOR THE CHAOTICALLY ORIENTED CIRCULAR CYLINDERS OF A FINITE LENGTH COMPARED WITH ANALOGOUS DATA FOR ELONGATED SPHEROIDS (ES)

Data for the chaotically oriented ES with  $a/b = 2$  and  $a/b = 5$  are taken from Ref. 8. The refractive index

$m = 1.33$  and  $k\alpha = 15$  in both cases, where  $k = 2\pi/\lambda$  is the wave number,  $\lambda$  is the wavelength of incident radiation. Elements of the scattering phase matrix for the chaotically oriented CCFL were calculated for two cases of  $l/d = 2.828$  and  $l/d = 7.071$ , the value  $kl$  being equal to 30 in both cases. Figure 1 shows the results for the CCFL with  $l/d = 7.071$  and for the ES with  $a/b = 5$ , while Fig. 2 shows the results for  $l/d = 2.828$  and  $a/b = 2$ . Data for the CCFL are shown by solid lines and the data for the ES are marked by triangles.

On the whole, the obtained results confirm that mostly the scattering phase matrix elements have similar features in both cases of the chaotically oriented CCFL and ES: the scattering phase matrix is symmetric; the phase function is quite smooth in the vicinity of the backward scattering direction;  $P_{22} \leq P_{11}$ ;  $P_{33} \neq P_{44}$ ; and  $P_{12} \leq 0$  for a certain size of particles and scattering angles while in the case of volume equivalent spheres  $P_{12} > 0$  at the same size and scattering angles.

At the same time there are certain specific peculiarities and differences from the case of the ES. Thus, for example,

- (a) The values of the matrix element  $P_{11}$  for the CCFL, which is the normalized scattering phase function for an unpolarized incident radiation (Figs. 1 *a* and 2 *a*) are very close to the values of this element for the ES while being qualitatively different from this element for volume equivalent spheres.

- (b) The quantity  $p = P_{12}/P_{11}$ , that determines the degree of linear polarization of radiation singly scattered by the randomly oriented CCFL in the case of unpolarized incident radiation and  $l/d = 7.071$  (Fig. 1 *b*) is very close to the degree of polarization in the case of the randomly oriented ES with  $a/b = 5$ . The elements  $p$  for the CCFL with  $l/d = 2.828$  and for the ES with  $a/b = 2$  (Fig. 2 *b*) have close values within the scattering angles  $0^\circ \leq \theta \leq 60^\circ$  and  $120^\circ \leq \theta \leq 180^\circ$ . Within the interval  $60^\circ < \theta < 120^\circ$  for the CCFL the quantity  $p$  becomes positive while for the ES it is either negative or positive but its positive values in this case are lower than the corresponding values for the CCFL. Similar situation can be seen from a comparison of  $p$  for the ES and the volume-equivalent spheres made in Ref. 8.

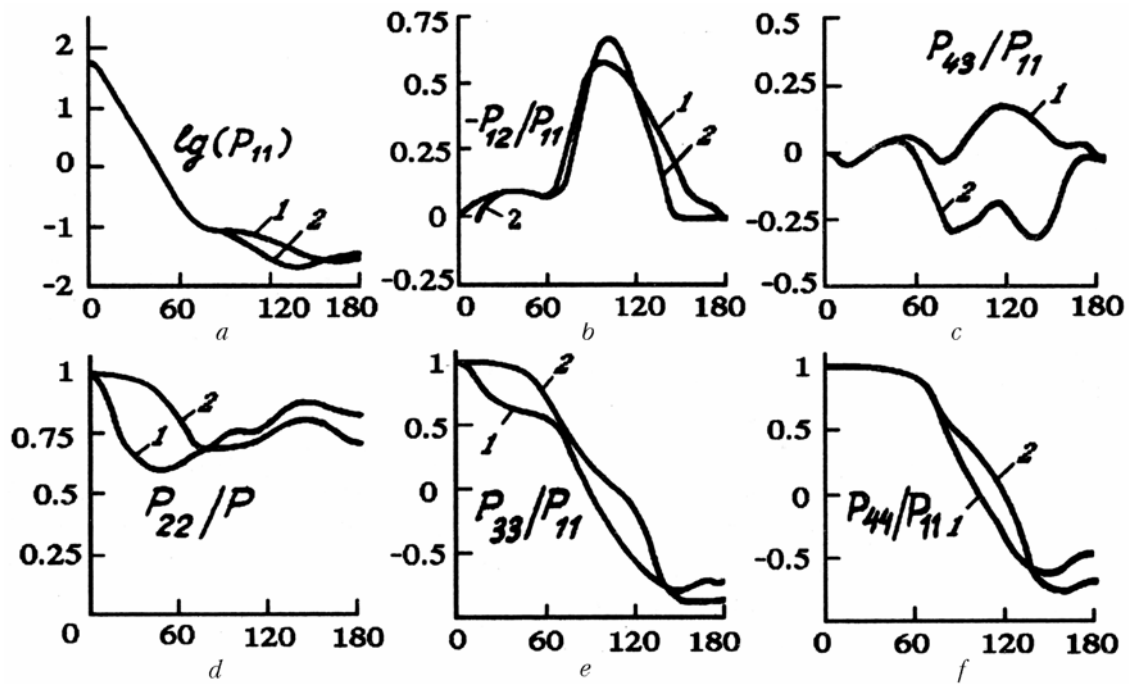


FIG. 1. The angular dependence of the normalized elements of a scattering phase matrix for randomly oriented circular cylinders of a finite length with  $l/d = 7.071$ ,  $kl = 30$  and elongated spheroids with  $a/b = 5$ ,  $m = 1.33$ , and  $ka = 15$ ; 1) cylinders and 2) spheroids.

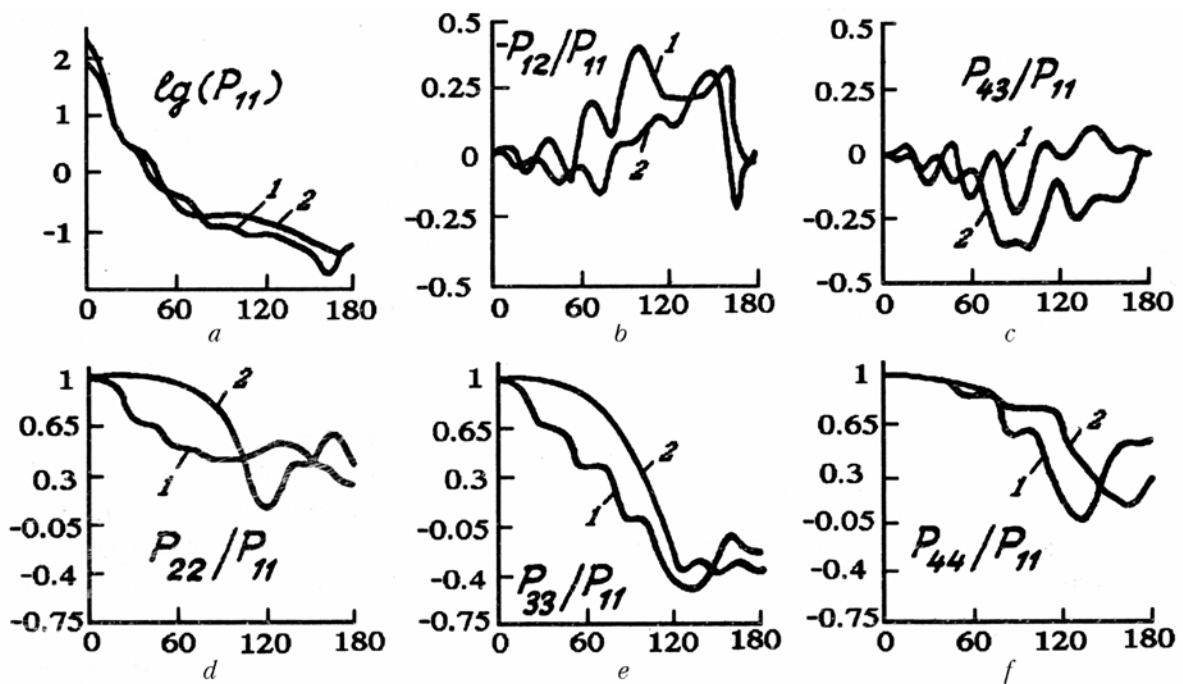


FIG. 2. The same as in Fig. 1, but for  $l/d = 2.282$  and  $a/b = 2$ . The designations of curves are the same as in Fig. 1.

(c) The depolarization ratio  $\Delta = (1 - P_{22}/P_{11})$  that characterizes the degree of nonsphericity of scattering particles is very small at the small angles (Figs. 1 *d* and 2 *d*) for the ES, while for the CCFL its values are essentially nonzero, what shows that the CCFL depolarizes a scattered light to a greater degree than the ES and spheres do at these angles. This conclusion well agrees with the experimental data on the scattering phase matrix elements for the cubic-shaped particles of sodium chloride.<sup>5</sup> This regularity, is more obviously observed in the experiments with aerosol particles of quartz flakes<sup>6</sup> the data of which are presented in the normalized form in Ref. 7. The values of  $\Delta$  for the CCFL with  $l/d = 7.071$  are close to the values of  $\Delta$  for the ES with  $a/b = 5$  at  $60^\circ \leq \theta \leq 180^\circ$  (Fig. 1 *d*). The largest value of  $\Delta$  is observed for the CCFL with  $l/d = 2.828$  and for the ES with  $a/b = 2$  at  $\theta \gg 90^\circ$ , what is determined, as will be shown in Section<sup>2</sup> of this paper, by the fact that the second critical dimension of a particle (for the CCFL it is  $r$  and for the ES —  $b$ ) is closer to the resonance region than for the case of the CCFL with  $l/d = 7.071$  and for the ES with  $a/b = 5$ .

(d) The ratio  $P_{43}/P_{11}$ . In the case of small scattering angles  $0^\circ \leq \theta \leq 60^\circ$  the value of this element for the CCFL is close to these for the ES (in both cases of particle elongation). Within the interval of scattering angles  $60^\circ \leq \theta \leq 180^\circ$  the value of this element for the CCFL is closer to the ratio  $P_{43}/P_{11}$  given in Ref. 8 for strongly oblate spheroids and to experimental data for the flake-shaped randomly oriented particles.<sup>6</sup> It can be assumed that small values of the ratio  $P_{43}/P_{11}$  at large scattering angles  $\theta > 90^\circ$  are due to larger curvature of nonspherical scattering particles. In the case of the CCFL the curvature of the particle surface is infinitely small along one dimension, while for strongly oblate spheroids the area of the surface with small radius of curvature is small compared to that of the surface portion with large radius of curvature. This can be well seen when one comes from the CCFL with  $l/d = 7.071$  (Fig. 1 *c*) to the CCFL with  $l/d = 2.828$  (Fig. 2 *c*).

(e) The ratio  $P_{33}/P_{11}$  and  $P_{44}/P_{11}$ . In the table the calculations show that  $(P_{11} - P_{22}) > (P_{44} - P_{33}) > 0$  for  $\theta > 4^\circ$  and  $\theta \neq 180^\circ$ . For  $0^\circ < \theta < 4^\circ$   $(P_{44} - P_{33}) < 0$ ;  $\theta = 0^\circ$   $(P_{11} - P_{22}) = -(P_{44} - P_{33})$  and  $P_{33} = P_{22}$ ;  $\theta = 180^\circ$   $(P_{11} - P_{22}) = (P_{44} - P_{33})$ ,  $P_{33} = -P_{22}$ , and the behavior of the difference  $P_{44} - P_{33}$  is almost the same as  $P_{11} - P_{22}$ , excluding the aureole part.

In conclusion of the comparative analysis let us note that the angular features of light scattering by the randomly oriented CCFL and the ES are very similar, and, moreover, this similarity gets stronger as the elongation  $l/d$  increases. The elongated spheroids, although different in scattering properties from spherical particles, are closer to the former than the CCFL whose scattering phase matrix elements better agree with the experimental data on chaotically oriented cubic<sup>5</sup> and flake-like<sup>6</sup> particles.

TABLE I.

$\theta$	$kl = 30, l/d = 7.071$		$kl = 30, l/d = 2.282$	
	$1 - \frac{P_{22}}{P_{11}}$	$\frac{P_{44} - P_{33}}{P_{11}}$	$1 - \frac{P_{22}}{P_{11}}$	$\frac{P_{44} - P_{33}}{P_{11}}$
0	0.00544	-0.00544	0.00178	-0.00178
2	0.00764	-0.00321	0.00263	-0.00089
4	0.01478	0.00403	0.00528	0.00189
6	0.02873	0.01825	0.01031	0.00717
10	0.08476	0.07591	0.03065	0.02861
20	0.25226	0.24713	0.10522	0.10107
30	0.33207	0.32827	0.32630	0.31958
35	0.36116	0.35769	0.35249	0.34822
40	0.37693	0.37355	0.34043	0.33758
50	0.38988	0.38630	0.38195	0.37634
65	0.35093	0.34510	0.50510	0.49839
80	0.29714	0.28725	0.56325	0.55400
100	0.29241	0.28206	0.58300	0.57649
120	0.23888	0.22928	0.50477	0.49948
135	0.18069	0.17154	0.46473	0.45991
141	0.17345	0.16488	0.51665	0.51165
150	0.18114	0.17423	0.60066	0.59661
160	0.21333	0.20961	0.63034	0.62740
165	0.23340	0.23121	0.67367	0.67149
171	0.26003	0.25918	0.72538	0.72470
179	0.28375	0.28373	0.75760	0.75759
180	0.28478	0.28478	0.75976	0.75976

## 2. THE DEPENDENCE OF DEPOLARIZATION CHARACTERISTICS OF BACKSCATTERING LIGHT ON DIELECTRIC PARAMETERS AND THE RADIUS OF CYLINDRIC SCATTERING PARTICLES

The components of the Stokes vector of radiation backscattered from the CCFL of soot and ice were calculated using the procedure proposed in Ref. 4 for the case of linearly polarized incident radiation with the wavelengths 1.06 and 10.6  $\mu\text{m}$ . The ensemble of the CCFL was taken to have a lognormal distribution of particles over the cross section radius with the parameters  $r_m = 0.1$ –16  $\mu\text{m}$  and  $\sigma_r = 0.1$  and 0.5; the distribution of the ratio of the cylinder length to its radius was assumed to be uniform over the interval 5–10 and the distribution of particle orientation angles  $\beta$  was assumed to be normal with  $\beta_m = 90^\circ$  and  $\sigma_\beta = 0.1$ ,  $\alpha = 45^\circ$ ; where  $\beta$  is the angle between the direction of incident radiation and the cylinder axis;  $\alpha$  is the angle between the plane of scattering and the plane containing the direction of incident radiation propagation and the axis of the cylinder. In all we considered four cases (Fig. 3):  $\lambda = 1.06 \mu\text{m}$ ,  $m = 1.299 - 0.0001i$ , and  $\sigma_r = 0.1$  (curve 1);  $\lambda = 1.06 \mu\text{m}$ ,  $m = 1.299 - 0.0001i$ , and  $\sigma_r = 0.5$  (curve 2);  $\lambda = 10.6 \mu\text{m}$ ,  $m = 2.2 - 0.093i$ , and  $\sigma_r = 0.1$  (curve 3);  $\lambda = 1.06 \mu\text{m}$ ,  $m = 1.91 - 0.68i$ , and  $\sigma_r = 0.1$  (curve 4).

Figure 3 *a* shows the intensity of backscattered radiation  $I$  normalized to unity. For all of the four cases  $I(r)$  fluctuates and decreases with  $r$ . More intense backscattering by absorbing particles occurs due to their optical hardness (the larger values of not only the imaginary but also real parts of the refractive index). Deeper and more frequent fluctuations are observed for the transparent particles with  $\sigma_r = 0.1$  (curve 1, Fig. 3 *a*) that, as is well known, is a result of the interference between the externally diffracted field with the field refracted by particles. Figure 3 *b* shows the second normalized component of the Stokes vector  $Q$ , which determines the degree of the linear polarization in the planes  $\varphi = 0^\circ$  and  $90^\circ$ . The depolarizing properties of crystalline media under consideration are well illustrated by the behavior of the curves. Thus, in particular, the absorbing particles possess the property to essentially transform the polarization of incident radiation when the modal radius  $r_m \leq \lambda$ , with degree of polarization of scattered light being close to unity. For transparent particles the polarization of scattered light when  $r_m \leq \lambda$  is close to that of the incident radiation. Absorbing particles do not possess depolarizing properties for

$r_m > \lambda$  (Fig. 3 *b*, curve 3 is for  $r_m > 10.6$ , curve 4 for  $r_m > 1.06$ ). The transparent CCFL's with radius  $\lambda < r_m < 10 \lambda$  essentially transforms the polarization of the initial signal within the interval (they even depolarizes it for certain  $r_m$ ). In addition, the depth of fluctuations  $Q$  is determined, to a considerable degree, by the width of the particle size distribution as can be vividly seen from a comparison of curves 1 and 2 in Fig. 3 *b*. Figures 3 *c* and *d* show the third and fourth normalized components of the Stokes vector  $U$  and  $V$ , respectively. The component  $U$  characterizes the degree of the linear polarization in the planes at angles of  $45^\circ$  and  $135^\circ$  and the component  $V$  – the degree of the circular polarization. Moderately absorbing small particles (curve 3 in Fig. 3 *c*) rotate the polarization of the initial signal towards the orientation plane of the cylinder axis more than others particles do. The return signal scattered by very fine strongly absorbing particles (curve 4 in Fig. 3 *d*) and by transparent particles when  $r_m \approx 2\lambda$  (curve 1 in Fig. 3 *d*) acquires the largest degree of the circular polarization and, in addition, the components  $U$  and  $Q$  are close to zero.

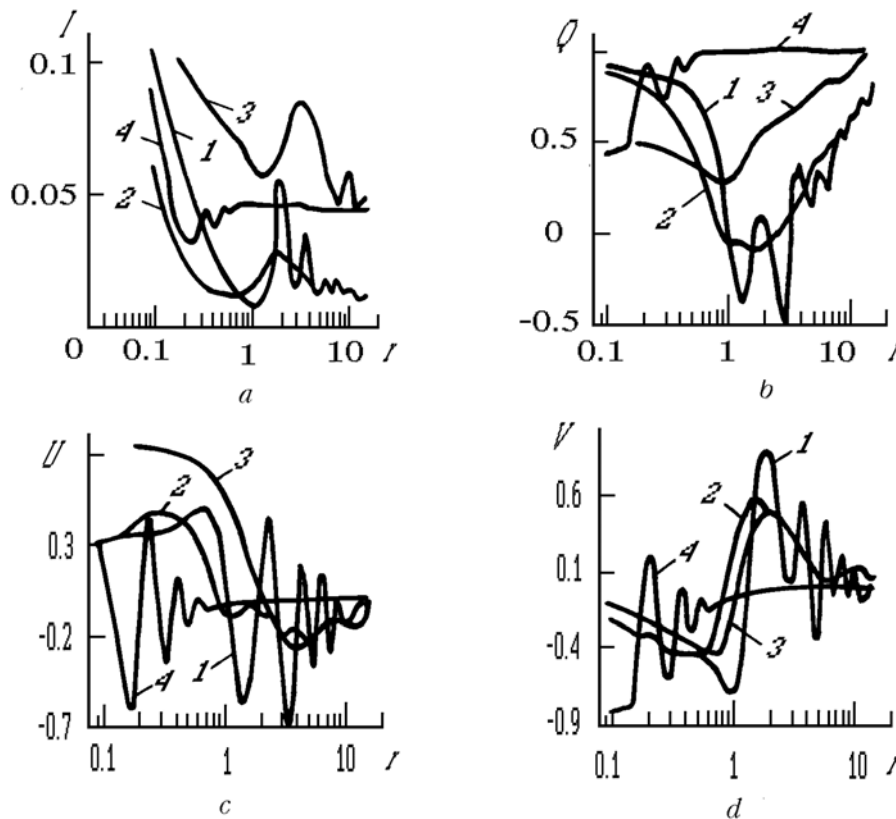


FIG. 3. Variation in the values of the Stokes vector components for backscattered radiation as a function of the modal radius  $r_m$ .

Thus, a strong dependence of depolarization properties of nonspherical scattering particles on the imaginary part of the refractive index of the particulate matter is observed. The effect of these properties on the backscattered radiation depends strongly on the width of the mode of the particle size distribution. There are cases ( $m$ ,  $r_m$ , and  $\alpha_r$ ) in which the ensembles of particles whose shapes strongly differ from the spherical ones possess the depolarizing properties for backscattering which are very close to those of spherical

particles. The behavior of curves 1 and 2 in Fig. 3 *b* shows that the depolarizing properties for elongated transparent particles are mostly determined not by the ratio of the maximum to minimum characteristic size of a particle (the aerodynamic cross section) but by the vicinity of one of them to the interval of resonance scattering. Difficulties which Asano and Sato<sup>8</sup> encountered in interpreting some of their results being "paradoxical" (at first sight) have apparently arisen just from ignoring this fact.

#### REFERENCES

1. S. Asano and G. Yamamoto, Appl. Opt. **14**, No. 1, 29–49 (1975).
2. P.C. Waterman, Phys. Rev. **23**, No. 4, 825–839 (1971).
3. O.A. Volkobitskii, L.N. Pavlov, and A.G. Petrushin, *Optical Properties of Crystal Clouds* (Gidrometeoizdat, Leningrad, 1984), 200 p.
4. R.F. Rakhimov and D.N. Romashov, Atm. Opt. **4**, No. 10, 707–710 (1991).
5. R.J. Perry, A.J. Hunt, and D.R. Huffman, Appl. Opt. **17**, No. 17 2700–2710 (1978).
6. A.C. Holland and G. Gange, Appl. Opt. **9**, No. 5, 1113–1121 (1967).
7. C.F. Bohren and D.R. Huffman, *Absorption and Scattering of Light by Small Particles* (Interscience–Wiley, New York, 1986).
8. S. Asano and M. Sato, Appl. Opt. **19**, No. 6, 962–974 (1980).